Addressing the problem of model dependency in GPD phenomenology

Paweł Sznajder
National Centre for Nuclear Research, Poland

2nd APCTP Workshop on the Physics of Electron Ion Collider,
Daegu, Republic of Korea, December 1st, 2023 (online participation)

Outline

- Introduction and motivation
- Double deeply virtual Compton scattering (DDVCS)
- Inclusion lattice-QCD results
- Machine learning techniques in GPD modelling
- Summary

Deeply Virtual Compton Scattering (DVCS)

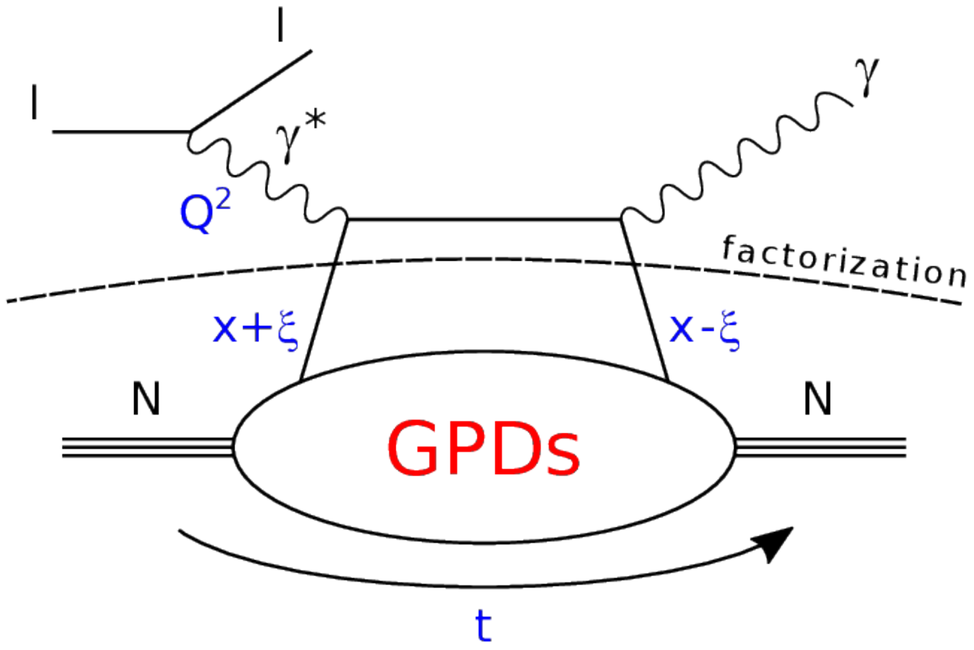

factorisation for $|t|/Q^2 \ll 1$

Chiral-even GPDs:
(helicity of parton conserved)

$H^{q,g}(x,\xi,t)$	$E^{q,g}(x,\xi,t)$	*for sum over parton helicities*
$\widetilde{H}^{q,g}(x,\xi,t)$	$\widetilde{E}^{q,g}(x,\xi,t)$	*for difference over parton helicities*
nucleon helicity conserved	*nucleon helicity changed*	

Introduction

Nucleon tomography:

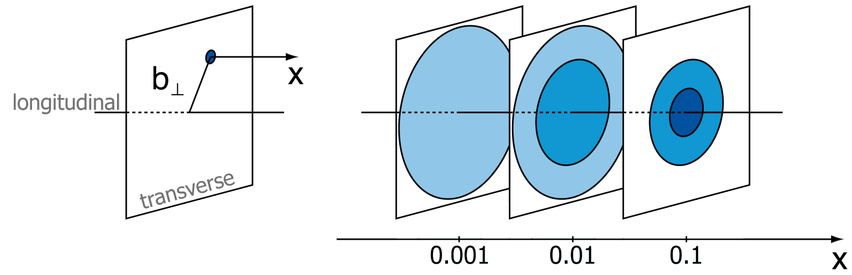

$$q(x,\mathbf{b}_\perp) = \int \frac{\mathrm{d}^2\boldsymbol{\Delta}}{4\pi^2} e^{-i\mathbf{b}_\perp\cdot\boldsymbol{\Delta}} H^q(x,0,t=-\boldsymbol{\Delta}^2)$$

Energy momentum tensor in terms of form factors (OAM and mechanical forces):

$$T^{\mu\nu} = \begin{bmatrix} T^{00} & T^{01} & T^{02} & T^{03} \\ T^{10} & T^{11} & T^{12} & T^{13} \\ T^{20} & T^{21} & T^{22} & T^{23} \\ T^{30} & T^{31} & T^{32} & T^{33} \end{bmatrix}$$

Energy density — Momentum density — Shear stress — Normal stress — Energy flux — Momentum flux

$$\langle p',s'|\widehat{T}^{\mu\nu}|p,s\rangle = \bar{u}(p',s')\left[\frac{P^\mu P^\nu}{M}A(t) + \frac{\Delta^\mu\Delta^\nu - \eta^{\mu\nu}\Delta^2}{M}C(t) + M\eta^{\mu\nu}\bar{C}(t) + \frac{P^\mu i\sigma^{\nu\lambda}\Delta_\lambda}{4M}[A(t)+B(t)+D(t)] + \frac{P^\nu i\sigma^{\mu\lambda}\Delta_\lambda}{4M}[A(t)+B(t)-D(t)]\right]u(p,s)$$

see Hyun-Chul Kim's talk

Total angular momentum:

$$A^q(0) + B^q(0) = \int_{-1}^{1} x\,[H^q(x,\xi,0) + E^q(x,\xi,0)] = 2J^q$$

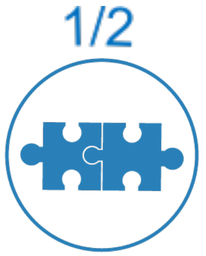

Ji's sum rule

"Mechanical" forces acting on quarks, e.g. pressure in nucleon center:

$$p(0) = \frac{1}{6\pi^2 M} \int_{-\infty}^{0} dt \sqrt{-t}\, t C(t)$$

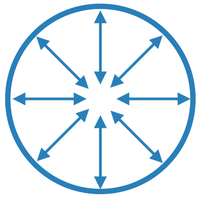

Introduction

GPDs accessible in various production channels and observables
→ experimental filters

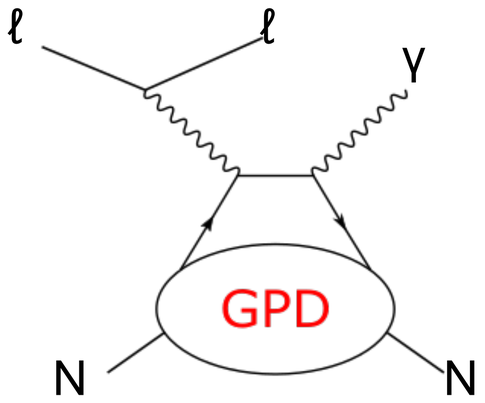

DVCS
Deeply Virtual Compton Scattering

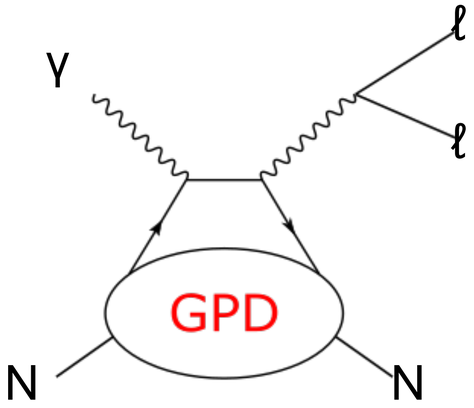

TCS
Timelike Compton Scattering

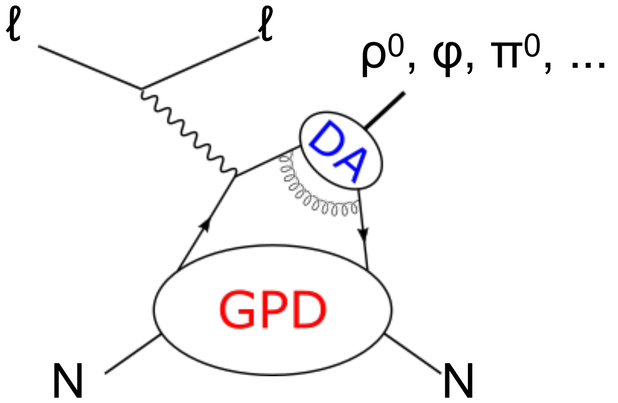

HEMP
Hard Exclusive Meson Production

more production channels sensitive to GPDs exist!

Shadow GPDs

V. Bertone et al.,
Phys. Rev. D 103 (2021) 11, 114019

Shadow GPDs have considerable size, but:

- at arbitrary initial scale do not contribute to PDFs and CFFs
- at other scales contribute negligibly

making the deconvolution of CFFs ill-posed problem

We found such GPDs for DVCS for both LO and NLO
(for discussion see also PRD 108 (2023) 3, 036027)

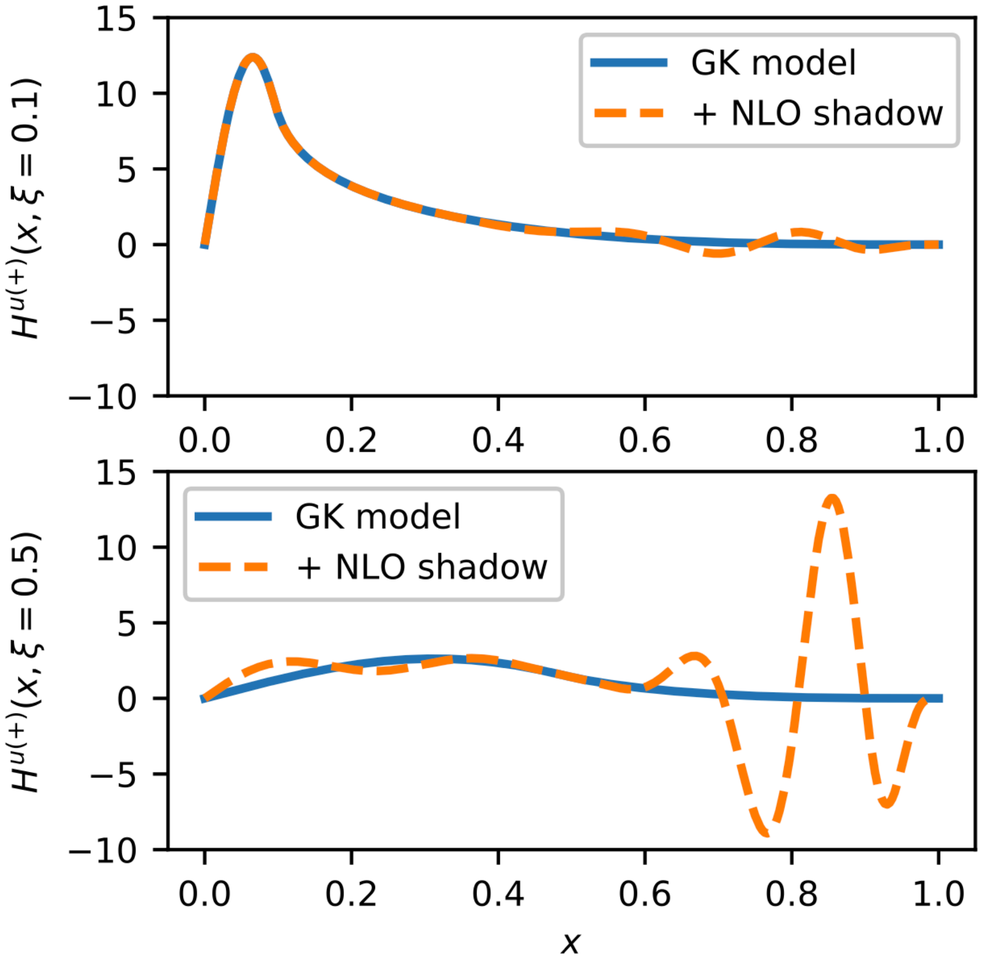

Exceptions

Studies less sensitive to model bias:

- probing nucleon tomography at low-xB (see: *PLB 793 (2019) 188*)

$$\mathrm{d}^3\sigma/(\mathrm{d}x_{\mathrm{Bj}}\,\mathrm{d}Q^2\,\mathrm{d}t) \propto (\mathrm{Im}\mathcal{H}(\xi,t))^2 \propto \left(\sum_q e_q^2 H^{q(+)}(\xi,\xi,t)\right)^2 \propto \left(\sum_q e_q^2 H^{q(+)}(\xi,0,t)\right)^2$$

- extraction of D-term (see: *Nature 570 (2019) 7759, E1*, *EPJC 81 (2021) 4, 300*)

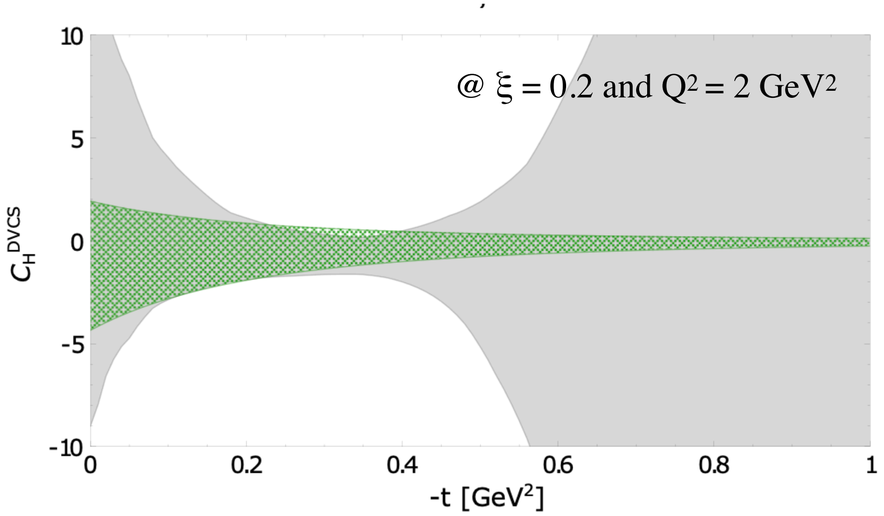

ANN analysis

Model dependent extraction

$$d_1^{uds}(t,\mu_F^2) = d_1^{uds}(\mu_F^2)\left(1-\frac{t}{\Lambda^2}\right)^{-\alpha}$$
$$\alpha = 3 \quad \Lambda = 0.8\ \mathrm{GeV}$$

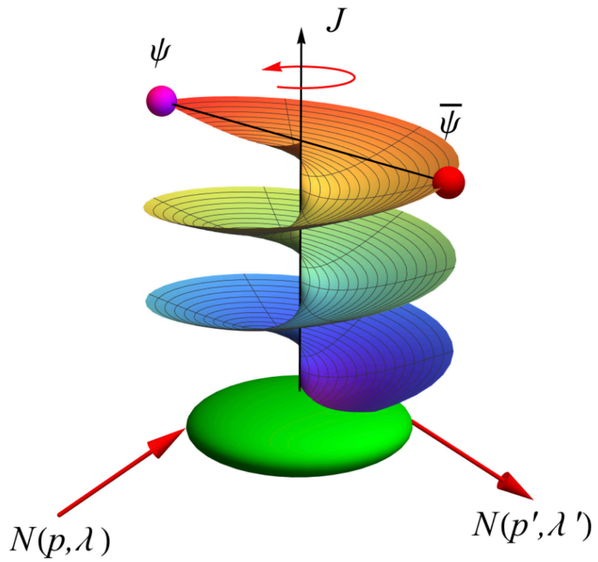

- Froissart-Gribov projections (see: *Kirill Semenov-Tian-Shansky's talk*)

Double DVCS

K. Deja, V. Martínez-Fernández,
B. Pire, PS, J. Wagner
Phys. Rev. D 107 (2023) 9, 094035

- The process allows to directly probe GPDs outside x=ξ line, but is much more challenging experimentally

$$(\mathcal{H},\mathcal{E})(\rho,\xi,t) = \sum_{f=\{u,d,s\}} \int_{-1}^{1} dx\; C_f^{(-)}(x,\rho)(H_f,E_f)(x,\xi,t)$$

$$C_f^{(\pm)}(x,\rho) \overset{LO}{=} \left(\frac{e_f}{e}\right)^2 \left(\frac{1}{\rho - x - i0} \pm \frac{1}{\rho + x - i0}\right)$$

$$\xi = \frac{Q^2 + Q'^2}{2Q^2/x_B - Q^2 - Q'^2}$$

$$\rho = \xi \frac{Q^2 - Q'^2}{Q^2 + Q'^2}$$

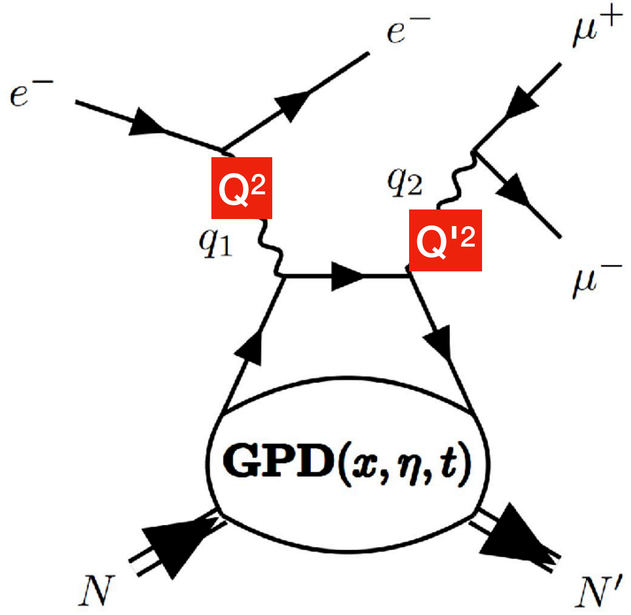

- We revisit DDVCS phenomenology in view of new experiments, including reevaluation of DDVCS and BH cross-sections with Kleiss-Stirling spinor techniques

- Obtained results are available in PARTONS and EpIC MC generator

Double DVCS

DVCS

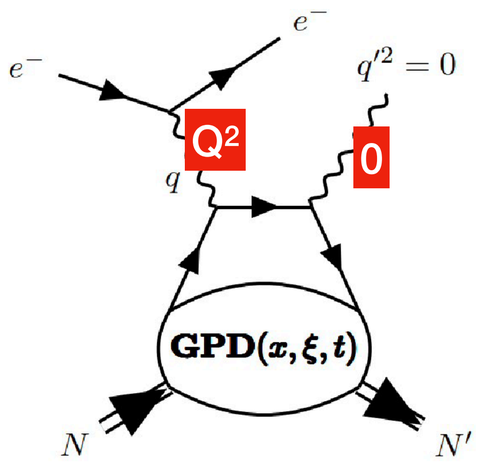

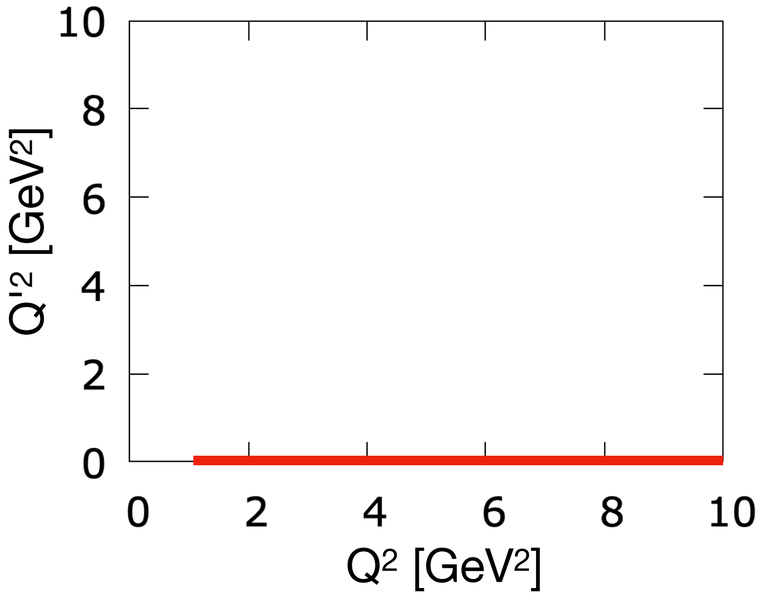

Double DVCS

DVCS

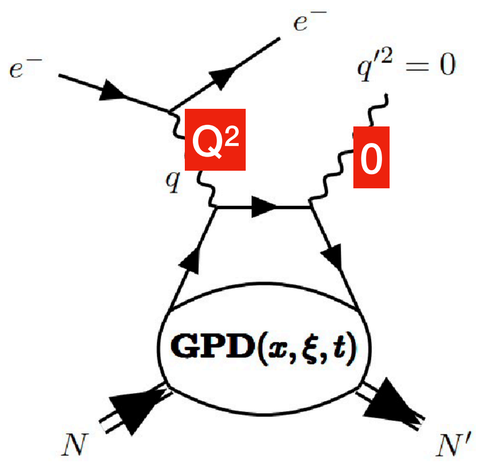

TCS

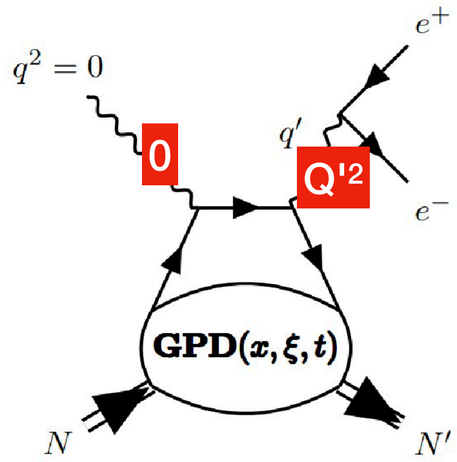

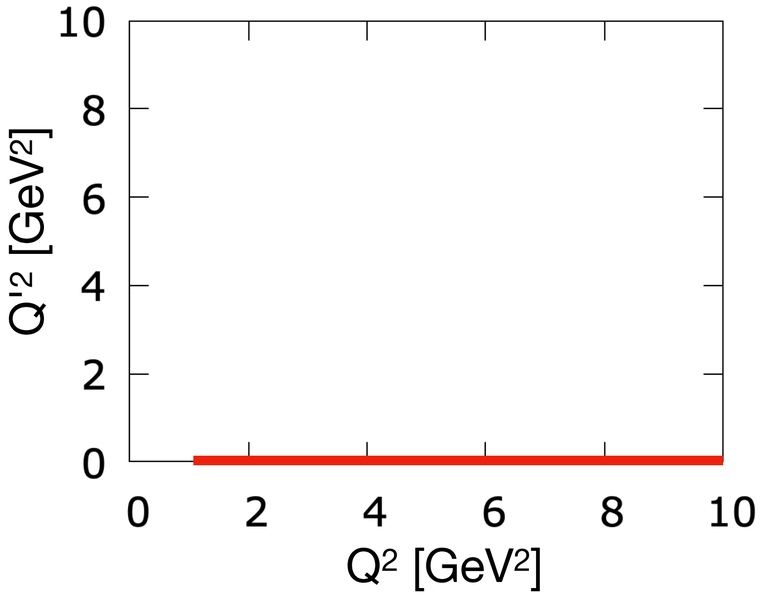

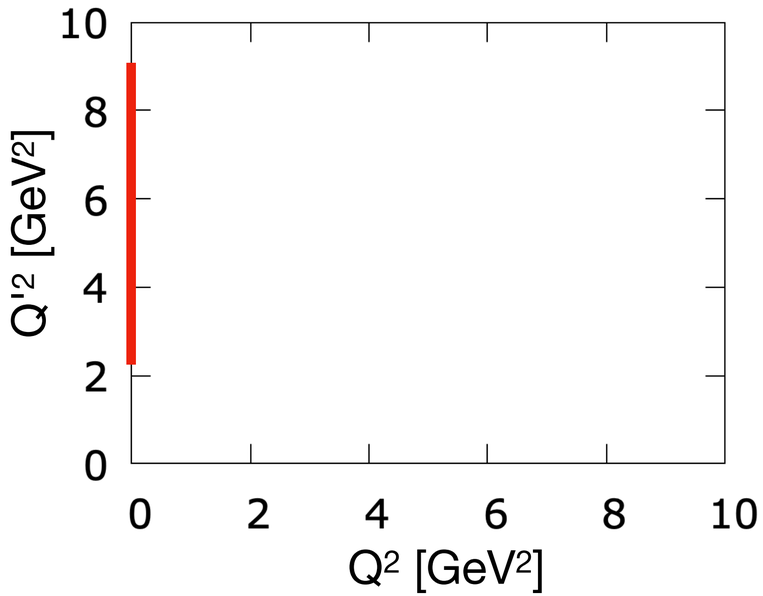

Double DVCS

DVCS

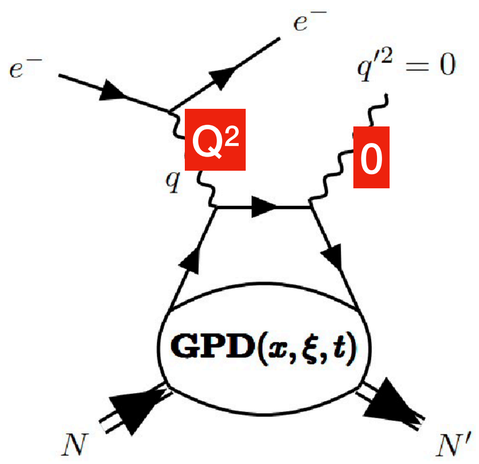

TCS in ep experiments

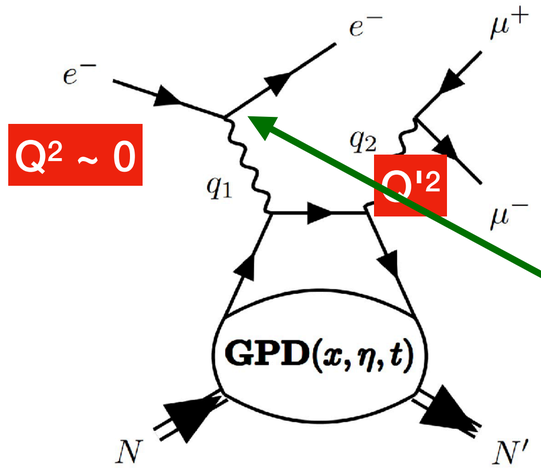

α_{EM} already here (in Γ)!

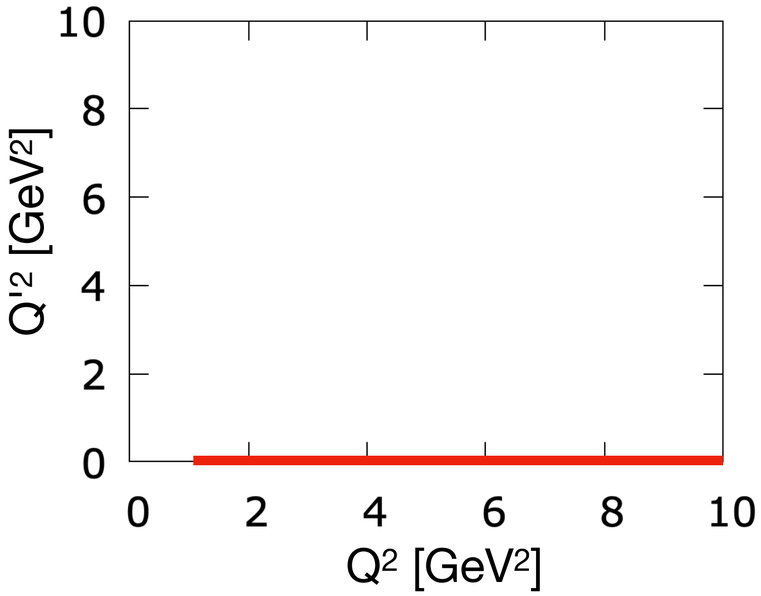

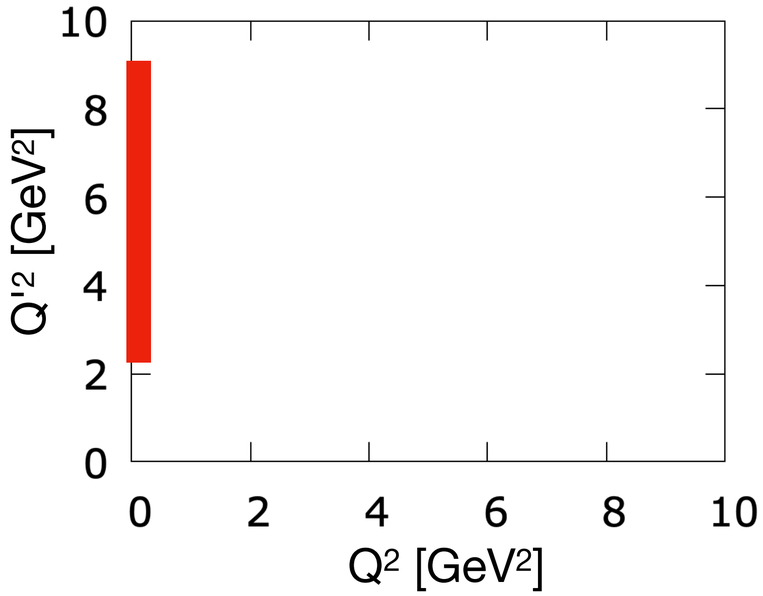

Double DVCS

DVCS

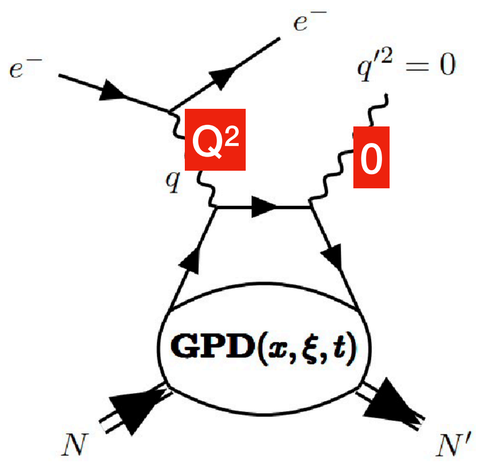

TCS in ep experiments

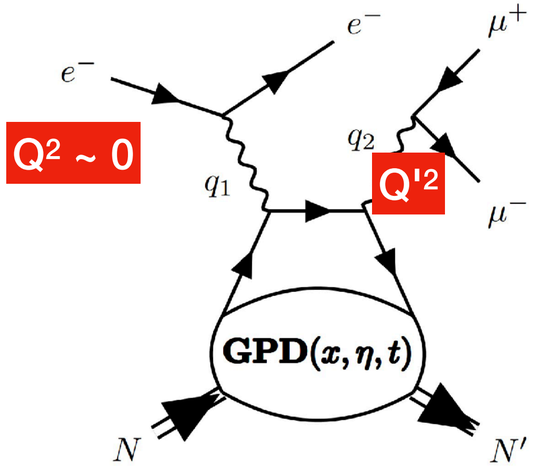

DDVCS

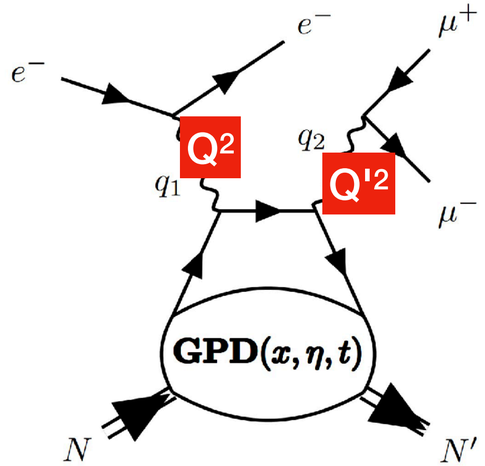

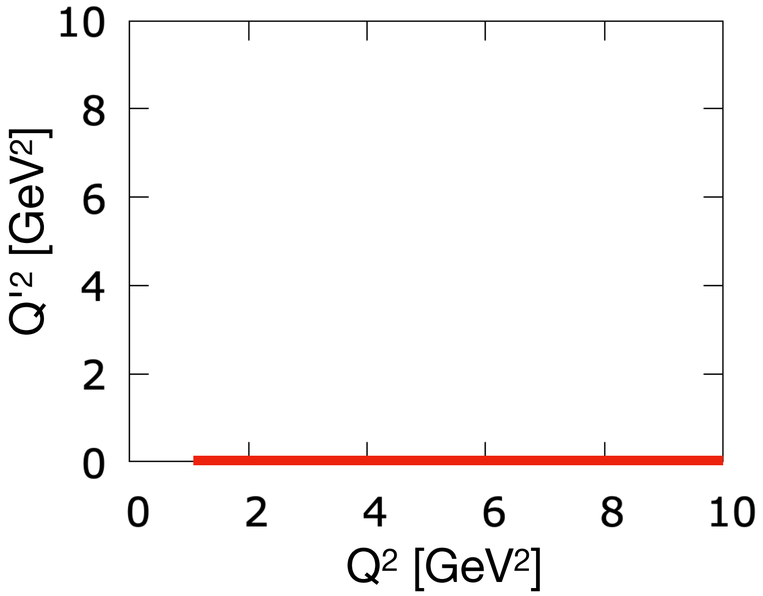

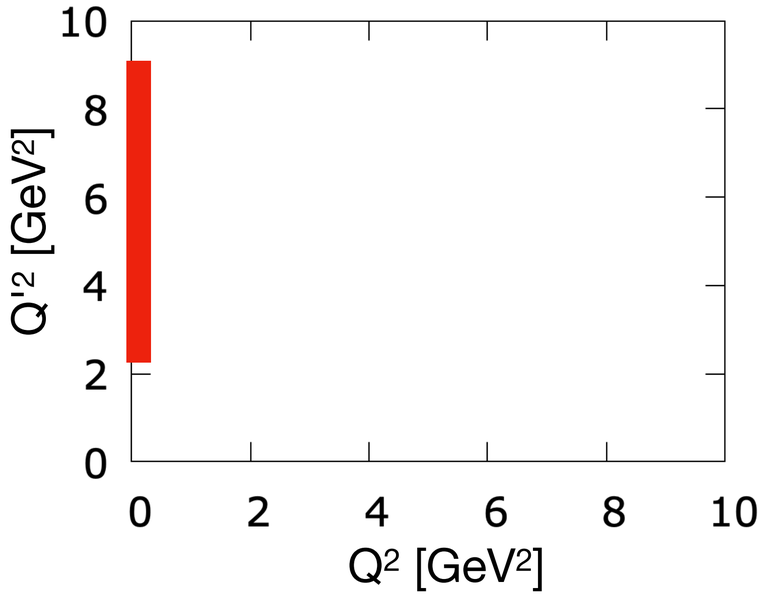

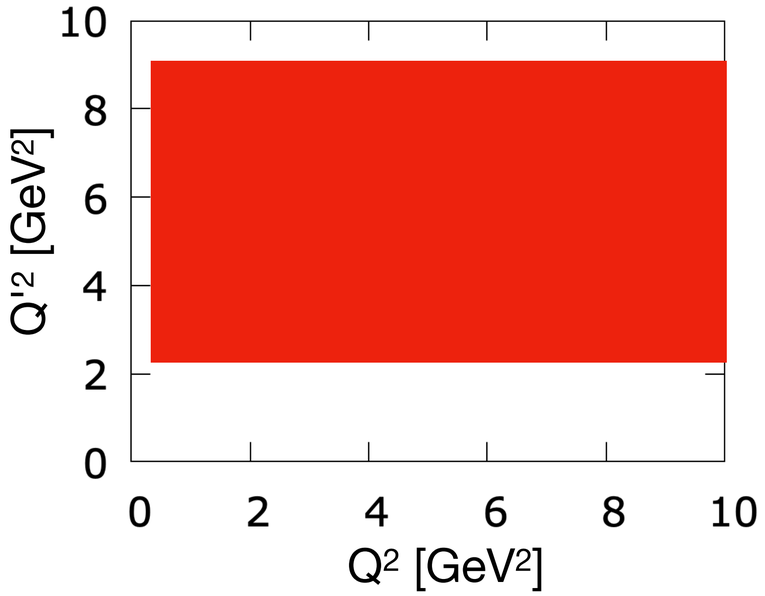

Double DVCS

K. Deja, V. Martínez-Fernández,
B. Pire, PS, J. Wagner
Phys. Rev. D 107 (2023) 9, 094035

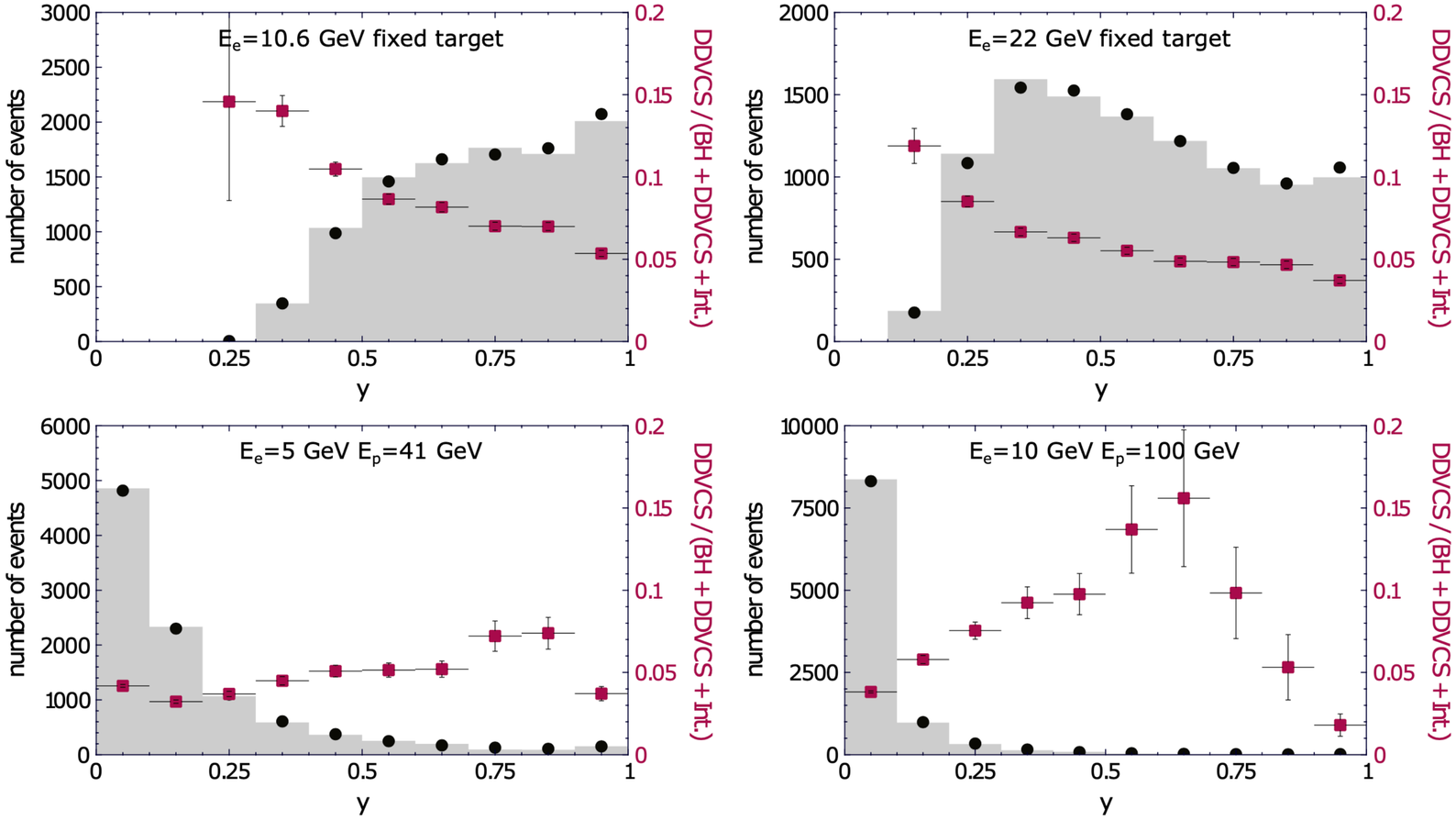

EpIC MC
integrated cross-section
pure DDVCS contribution

Kinematic cuts:

- 0.15 GeV^2 < Q^2 < 5 GeV^2
- 2.25 GeV^2 < Q'^2 < 9 GeV^2
- 0.1 GeV^2 < t < 0.8 GeV^2 (JLab)
- 0.05 GeV^2 < t < 1 GeV^2 (EIC)
- $0.1 < \varphi, \varphi_l < 2\pi - 0.1$
- $\pi/4 < \theta_l < 3\pi/4$
- 0.1 < y < 1 (JLab)
- 0.05 < y < 1 (EIC)

Experiment	Beam energies [GeV]	Range of $\lvert t\rvert$ [GeV^2]	$\sigma\lvert_{0<y<1}$ [pb]	$\mathcal{L}^{10k}\lvert_{0<y<1}$ [fb^{-1}]	$y_{\min}$	$\sigma\lvert_{y_{\min}<y<1}/\sigma\lvert_{0<y<1}$
JLab12	$E_e = 10.6,\ E_p = M$	$(0.1, 0.8)$	0.14	70	0.1	1
JLab2+	$E_e = 22,\ E_p = M$	$(0.1, 0.8)$	0.46	22	0.1	1
EIC	$E_e = 5,\ E_p = 41$	$(0.05, 1)$	3.9	2.6	0.05	0.73
EIC	$E_e = 10,\ E_p = 100$	$(0.05, 1)$	4.7	2.1	0.05	0.32

Double DVCS

K. Deja, V. Martínez-Fernández,
B. Pire, PS, J. Wagner
Phys. Rev. D 107 (2023) 9, 094035

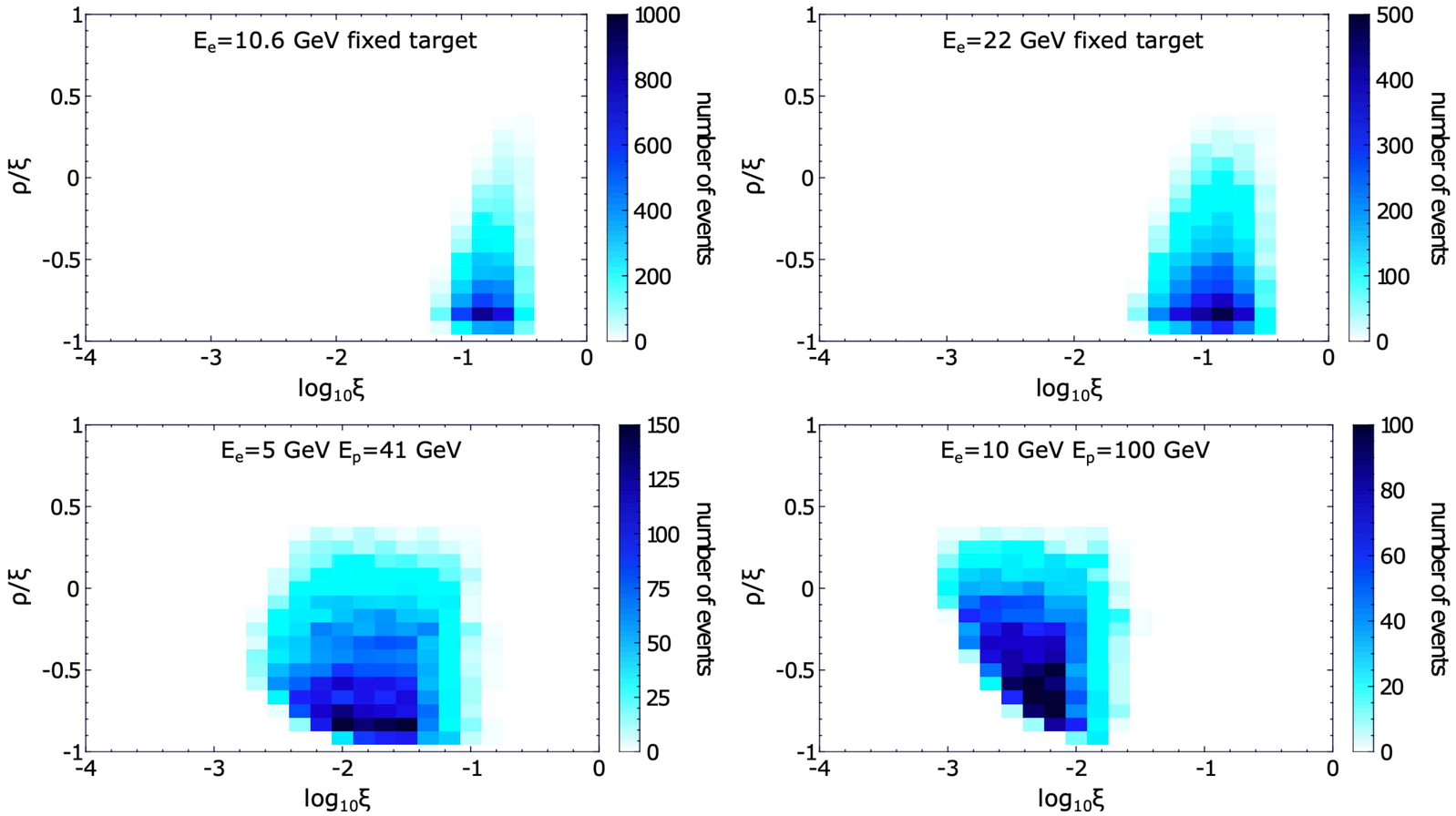

Kinematic cuts:

- $0.15\ \text{GeV}^2 < Q^2 < 5\ \text{GeV}^2$
- $2.25\ \text{GeV}^2 < Q'^2 < 9\ \text{GeV}^2$
- $0.1\ \text{GeV}^2 < t < 0.8\ \text{GeV}^2$ (JLab)
- $0.05\ \text{GeV}^2 < t < 1\ \text{GeV}^2$ (EIC)
- $0.1 < \varphi, \varphi_l < 2\pi - 0.1$
- $\pi/4 < \theta_l < 3\pi/4$
- $0.1 < y < 1$ (JLab)
- $0.05 < y < 1$ (EIC)

Double DVCS

K. Deja, V. Martínez-Fernández,
B. Pire, PS, J. Wagner
Phys. Rev. D 107 (2023) 9, 094035

Unpolarised cross-section integrated over $0 < \phi < 2\pi$ and $\pi/4 < \theta l < 3\pi/4$

corresponding ALU asymmetry

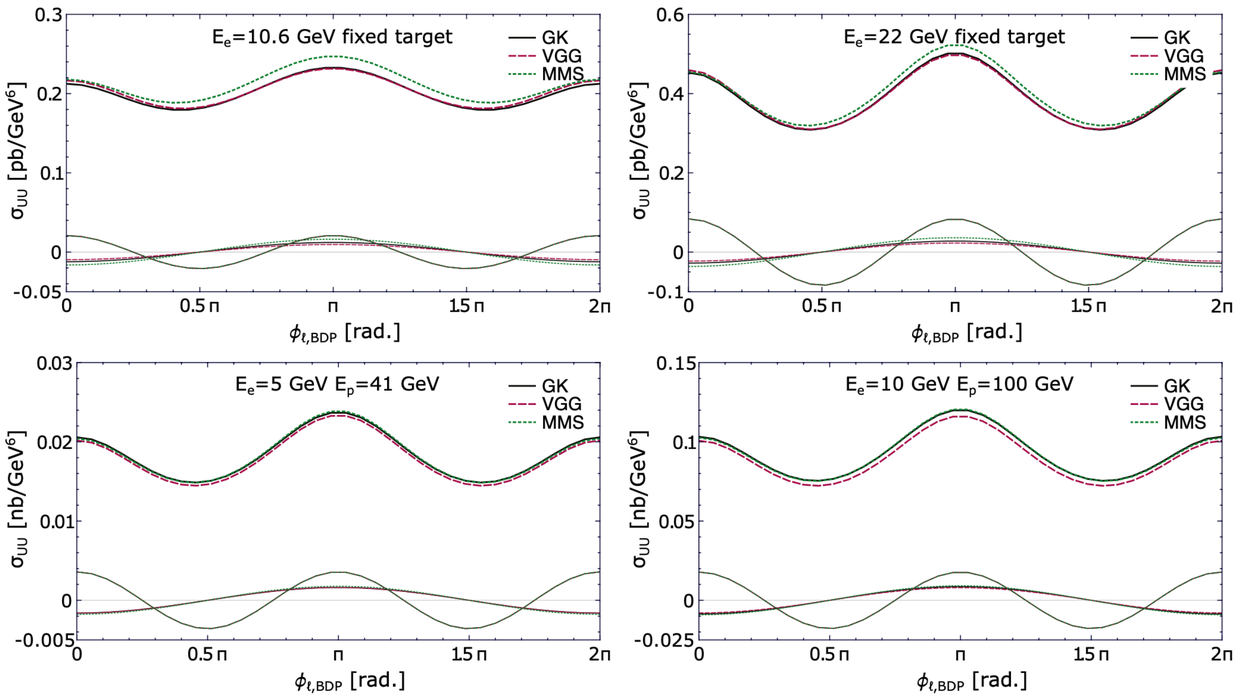

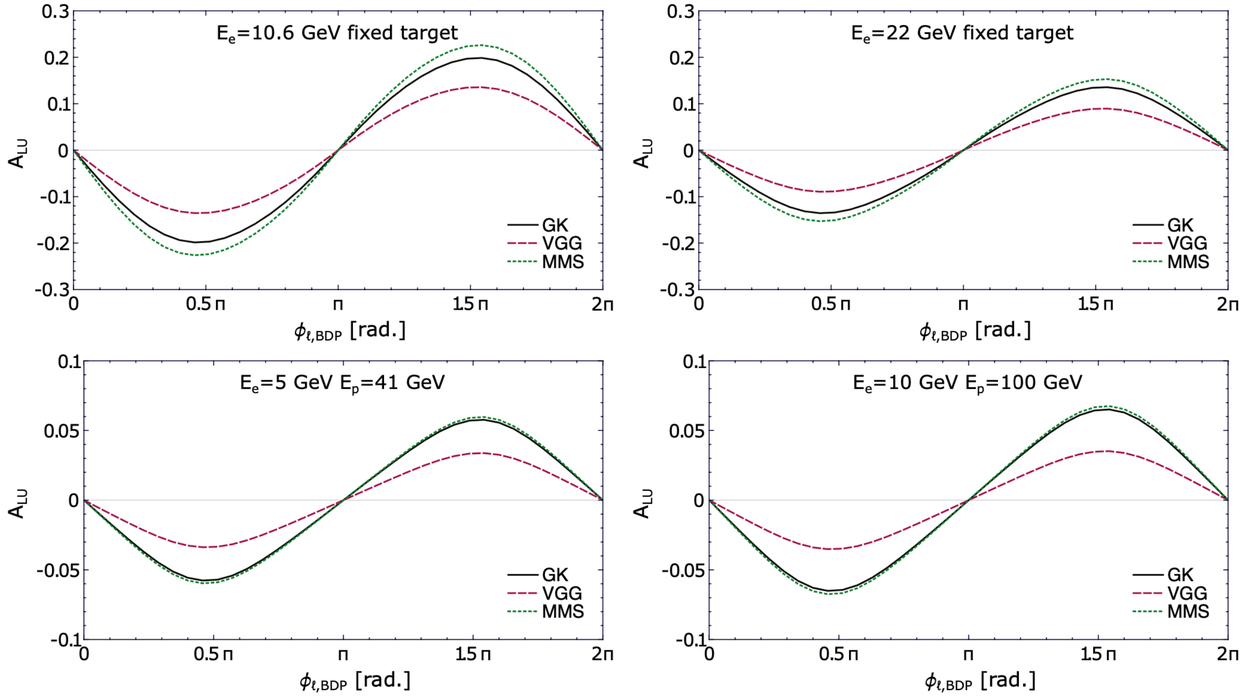

GK
VGG
MMS

Experiment	Beam energies [GeV]	y	$\lvert t\rvert$ [GeV^2]	Q^2 [GeV^2]	Q'^2 [GeV^2]
JLab12	$E_e = 10.6,\ E_p = M$	0.5	0.2	0.6	2.5
JLab2+	$E_e = 22,\ E_p = M$	0.3	0.2	0.6	2.5
EIC	$E_e = 5,\ E_p = 41$	0.15	0.1	0.6	2.5
EIC	$E_e = 10,\ E_p = 100$	0.15	0.1	0.6	2.5

Lattice-QCD

M. J. Riberdy, H. Dutrieux, C. Mezrag, PS, hep-ph/2306.01647

- Exploratory study to include lattice-QCD results!

Reduction of GPD model uncertainties due to inclusion of pseudo-latticeQCD results

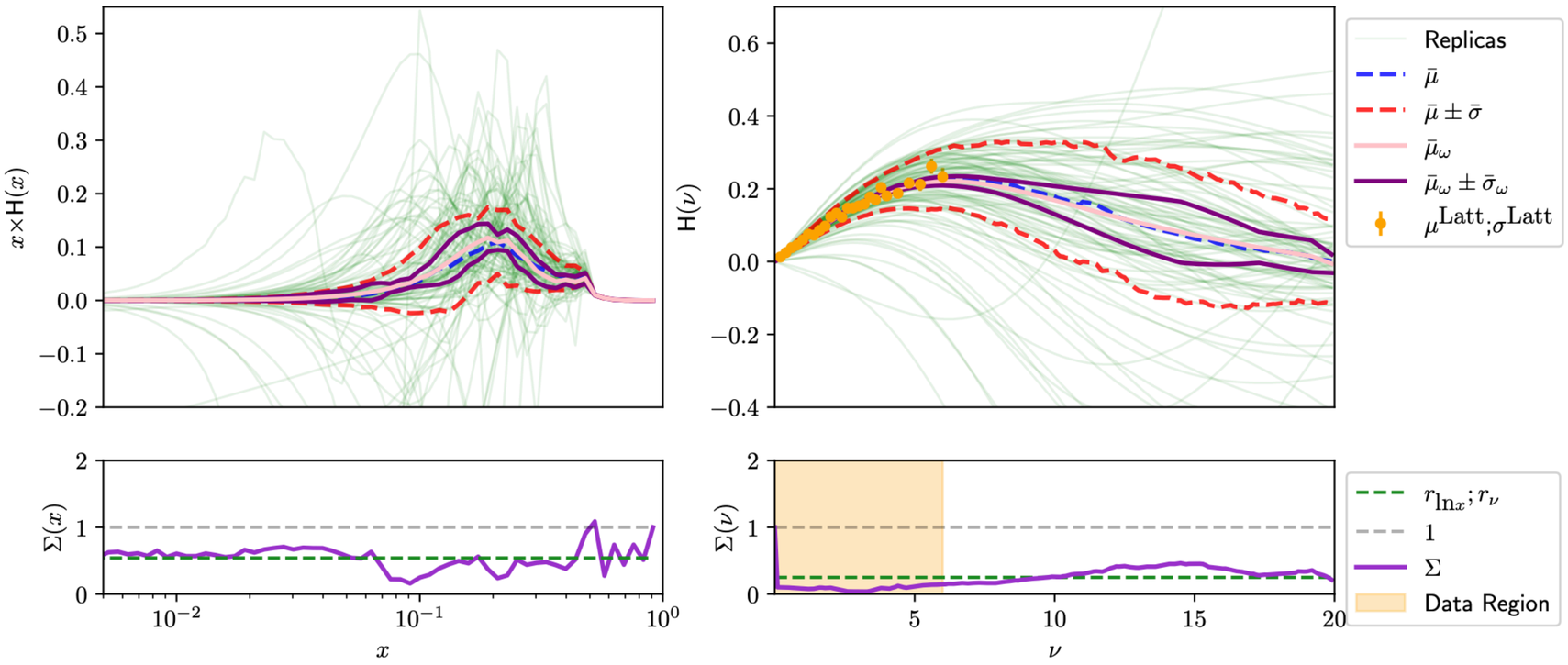

Double distribution:

$$H(x,\xi,t) = \int \mathrm{d}\Omega\, F(\beta,\alpha,t)$$

where:

$$\mathrm{d}\Omega = \mathrm{d}\beta\,\mathrm{d}\alpha\,\delta(x-\beta-\alpha\xi)$$

$$|\alpha| + |\beta| \leq 1$$

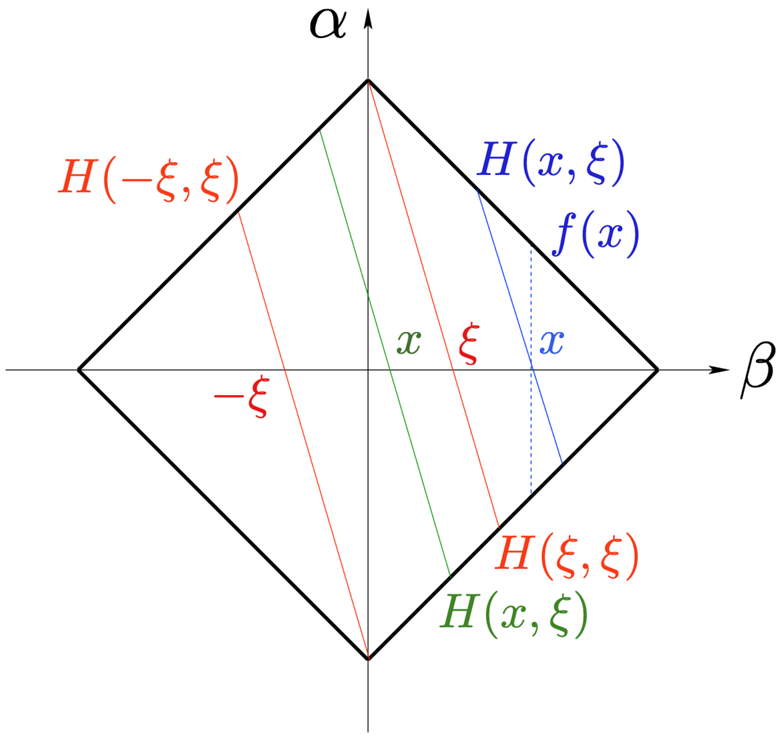

from PRD83, 076006, 2011

Principles of modelling

H. Dutrieux et al.,
Eur. Phys. J. C 82 (2022) 3, 252

Double distribution:

$$(1-x^2)F_C(\beta,\alpha)+(x^2-\xi^2)F_S(\beta,\alpha)+\xi F_D(\beta,\alpha)$$

Classical term:

$$F_C(\beta,\alpha)=f(\beta)h_C(\beta,\alpha)\frac{1}{1-\beta^2}$$

$$f(\beta)=\mathrm{sgn}(\beta)q(|\beta|)$$

$$h_C(\beta,\alpha)=\frac{\mathrm{ANN}_C(|\beta|,\alpha)}{\int_{-1+|\beta|}^{1-|\beta|}\mathrm{d}\alpha\mathrm{ANN}_C(|\beta|,\alpha)}$$

Shadow term:

$$F_S(\beta,\alpha)=f(\beta)h_S(\beta,\alpha)$$

$$f(\beta)=\mathrm{sgn}(\beta)q(|\beta|)$$

$$h_S(\beta,\alpha)/N_S=\frac{\mathrm{ANN}_S(|\beta|,\alpha)}{\int_{-1+|\beta|}^{1-|\beta|}\mathrm{d}\alpha\mathrm{ANN}_S(|\beta|,\alpha)}-\frac{\mathrm{ANN}_{S'}(|\beta|,\alpha)}{\int_{-1+|\beta|}^{1-|\beta|}\mathrm{d}\alpha\mathrm{ANN}_{S'}(|\beta|,\alpha)}.$$

$$\mathrm{ANN}_{S'}(|\beta|,\alpha)\equiv\mathrm{ANN}_C(|\beta|,\alpha)$$

D-term:

$$F_D(\beta,\alpha)=\delta(\beta)D(\alpha)$$

$$D(\alpha)=(1-\alpha^2)\sum_{\substack{i=1\\ \mathrm{odd}}}d_iC_i^{3/2}(\alpha)$$

H. Dutrieux et al.,
Eur. Phys. J. C 82 (2022) 3, 252

Our ANNs:

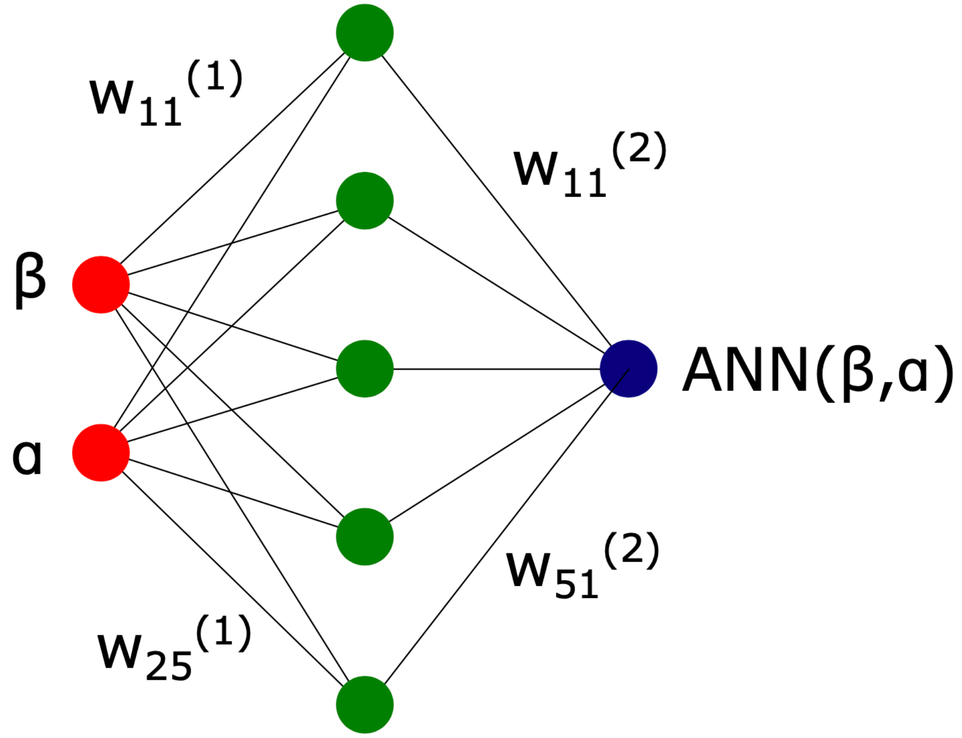

Requirements:

symmetric w.r.t. α

symmetric w.r.t. β

vanishes at $|\alpha| + |\beta| = 1$

Activation function:

$$\left(\varphi_i\left(w_i^{\beta}|\beta| + w_i^{\alpha}\alpha/(1-|\beta|) + b_i\right) - \varphi_i\left(w_i^{\beta}|\beta| + w_i^{\alpha} + b_i\right)\right) + (w^{\alpha} \to -w^{\alpha})$$

Demonstration of results

H. Dutrieux et al.,
Eur. Phys. J. C 82 (2022) 3, 252

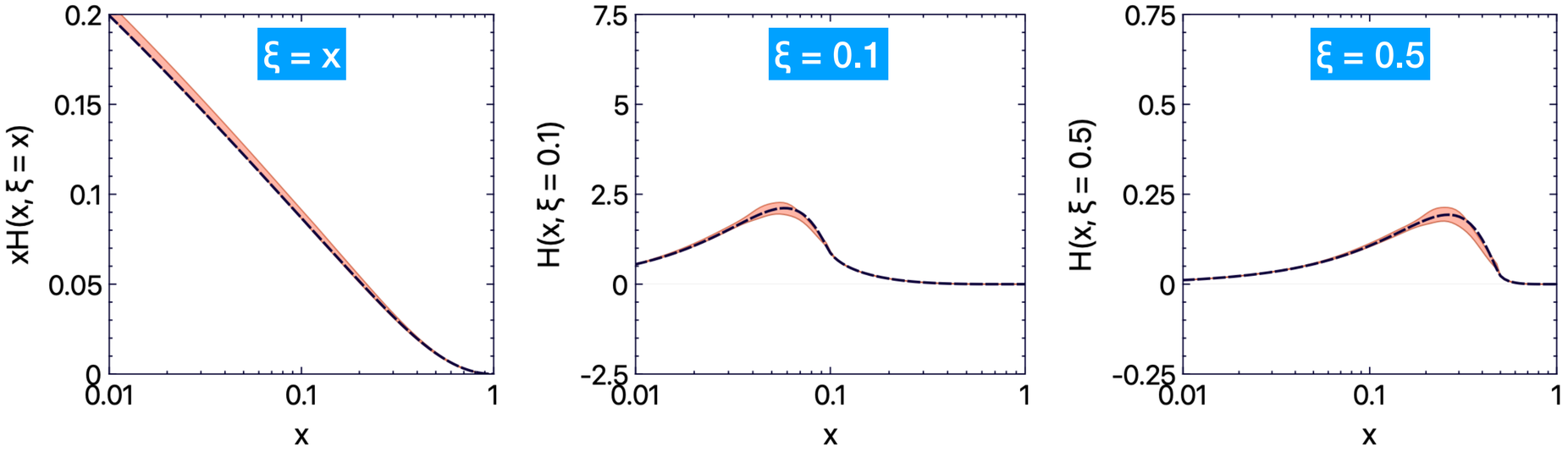

Conditions:

- Input: 400 $x \neq \xi$ points generated with GK model
- Positivity not forced

Technical detail of the analysis:

- Minimisation with genetic algorithm
- Replication for estimation of model uncertainties
- “Local” detection of outliers
- Dropout algorithm for regularisation

GK

ANN model
68% CL
$F_C + F_S + F_D$

Demonstration of results

H. Dutrieux et al.,
Eur. Phys. J. C 82 (2022) 3, 252

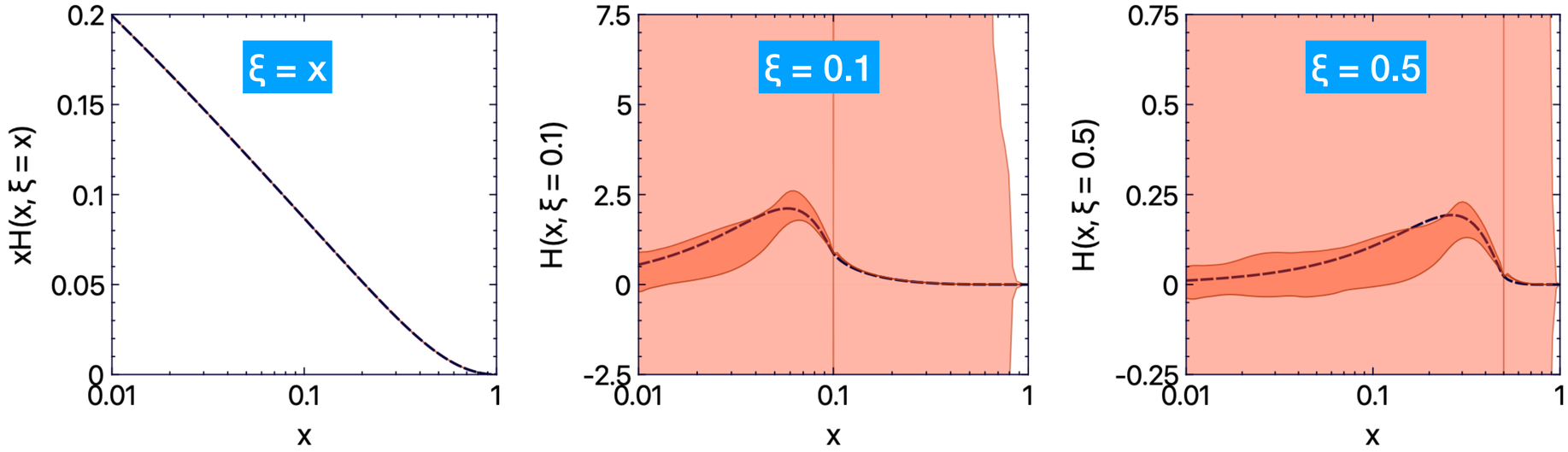

GK

ANN model
68% CL
F_C

ANN model
68% CL
$F_C + F_S$

Conditions:

- Input: 200 x = ξ points generated with GK model
- Positivity not forced

Demonstration of results

H. Dutrieux et al.,
Eur. Phys. J. C 82 (2022) 3, 252

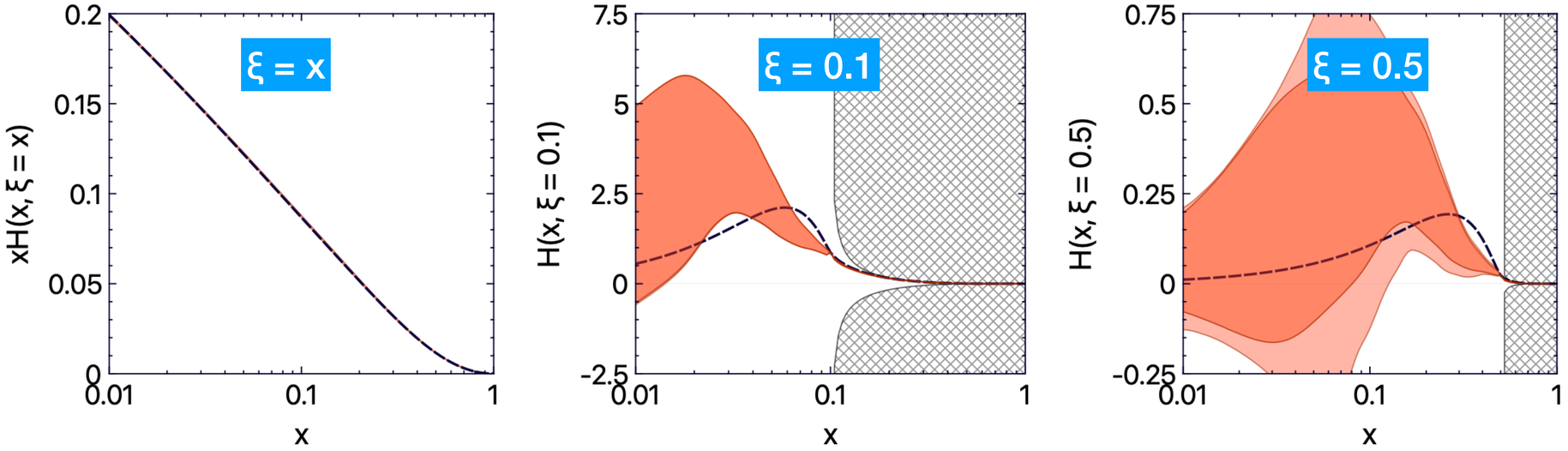

Conditions:

- Input: 200 x = ξ points generated with GK model
- Positivity **forced**

GK

ANN model 68% CL F_C

Excluded by positivity

ANN model 68% CL $F_C + F_S$

Summary

- Recent progress in:
  - understanding of fundamental problems, like deconvolution of CFFs
    → important for extraction of GPDs
  - description of exclusive processes
    → new sources of GPD information
  - modelling of GPD, fulfilling all theory-driven constraints (including positivity)
    → subject not touched enough in the current literature
    → developed in mind for easy inclusion of latticeQCD data
- Up next:
  - Practical use of new modelling techniques → multichannel GPD fits
  - Inclusion of real lattice-QCD results
  - Higher-twist corrections to DDVCS